



Original Research Article

***Emblica officinalis* leaf extract mediated synthesis of zinc oxide nanoparticles for antibacterial and photocatalytic activities**

Anbuvarannan Mari^{a,*}, Ramesh Mookkaiah^b, Manikandan Elayaperumal^c^a Department of Physics, Sri Akilandeswari Women's College, Wandiwash-604408, Tamil Nadu, India^b Department of Physics, M.V. Muthiah Government Arts College for Women, Dindigul- 624 001. Tamil Nadu, India^c Department of Physics, Thiruvalluvar University College of Arts & Science, Thennangur-604408. Tamil Nadu, India**ARTICLE INFORMATION**

Received: 18 September 2018

Received in revised: 18 October 2018

Accepted: 23 October 2018

Available online: 12 January 2019

DOI: [10.33945/SAMI/AJGC.2019.4.1](https://doi.org/10.33945/SAMI/AJGC.2019.4.1)**KEYWORDS**

Zinc oxide

Biosynthesis

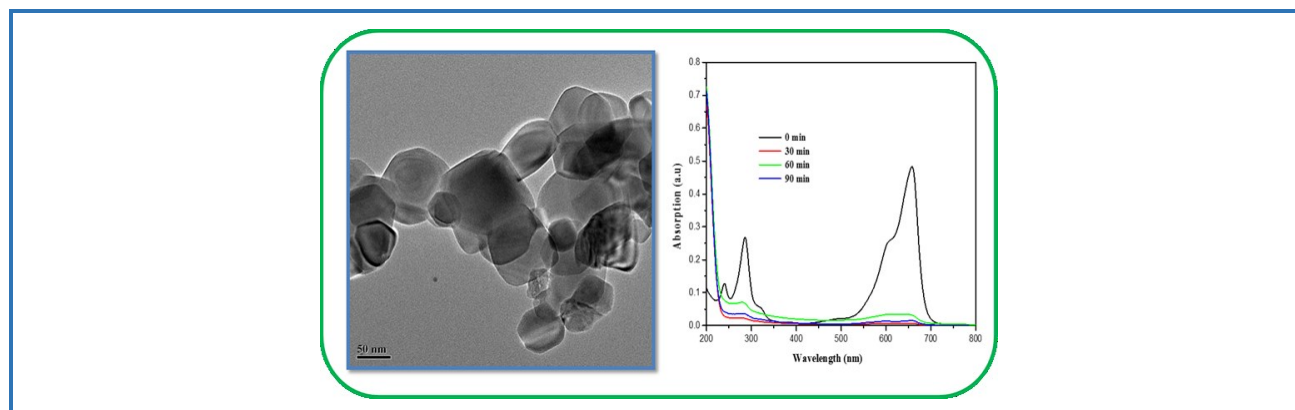
Photocatalysis

Antibacterial activity

ABSTRACT

In this work, ZnO nanoparticles were synthesized *via* a simple green method using just plant extract. The synthesized ZnO nanoparticles were characterized using UV-vis diffuse reflectance spectroscopy (UV-vis DRS), photoluminescence measurements (PL), X-ray diffraction (XRD), Fourier transform infrared spectroscopy (FT-IR), field emission scanning electron microscopy (FE-SEM), and transmission electron microscopy (TEM). Photocatalytic activities of the ZnO nanoparticles were evaluated by degradation of methylene blue under UV radiation. Moreover, the antibacterial activity of the synthesized ZnO nanoparticles against *S. aureus*, *S. paratyphi*, *V. cholerae*, and *E. coli* were screened.

© 2019 by SPC (Sami Publishing Company), Asian Journal of Green Chemistry, Reproduction is permitted for noncommercial purposes.

Graphical Abstract

Introduction

Semiconductor materials in nano dimensions have fascinated the scientific community in the recent past owing to their peculiar physical and chemical properties [1]. Among the semiconductor materials, ZnO as an important II–VI semiconductor material with a wide band gap of 3.37 eV and a large excitation binding energy of 60 MeV has been extensively studied due to its potential applications in ultraviolet light-emitting and laser diodes [2], field emission displays [3], solar cells [4], sensors [5, 6], varistors [7], and catalysis [8].

The synthesis of metal and metal oxide nanoparticles have attracted considerable attention from the physical, chemical, biological, medical, optical, mechanical, and engineering sciences. The metal oxides have high fraction of atoms and are responsible for their fascinating properties such as antimicrobial, magnetic, electronic, and catalytic activity [9].

Biosynthesis of ZnO NPs by plants such as *Aloe barbadensis* miller leaf [10], brown marine macro alga *Sargassum muticum* [11], seaweeds of gulf of Mannar [12], *Aeromonas hydrophila* [13], *Parthenium hysterophorus* [14], *Abrus precatorius* seeds [15], *Calotropis gigantea* [16], *Citrus aurantifolia* [17], *Ocimum sanctum* [18], Maple leaf [19], *Tamarindus indica* [20], *Solanum nigrum* [21], *Anisochilus carnosus* [22], *Phyllanthus niruri* [23] have been reported. Recently, green synthesis of NPs was achieved using microorganisms, plant extract due to its availability, low cost, non-toxic, biodegradable, and environment friendly characteristics. *Emblica officinalis* commonly known as *nellikai*, is a member of a small genus *Emblica* (Euphorbiaceae). It grows in tropical and subtropical parts of China, India, Indonesia and the Malay Peninsula. All parts of the plant are used for medicinal purpose.

Emblica exhibits strong antioxidant activities, and it is one of the most important plants in the traditional Ayurvedic medical system. It is also used as immunomodulatory, anti-inflammatory, antiulcer, hepatoprotective, and anticancer actions in other traditional health systems. Chemical constituents of this plant are flavonoids, kaempferol, ellagic acid, gallic acid [24], pyrogallol, norsesquiterpenoids, corilagin, geraniin, elaeocarpusin, prodelphinidins B₁, and B₂.

In this research study, we demonstrate a green method to synthesize ZnO-NPs. For the preparation, zinc nitrate and leaf extract of *Emblica officinalis* at different proportions were used. The synthesized NPs were characterized using UV-DRS, PL, FT-IR, XRD, FE-SEM, and TEM. The photocatalytic and antibacterial activities of the ZnO have also been studied.

Experimental

Preparation of the leaf extract

Plant leaves of *Emblica Officinalis* were collected from Polur, Tiruvannamalai District, Tamil Nadu, and India. The collected leaves were washed several times with distilled water to remove the dust particles. 20 g of fine cut leaves in 250 mL glass beaker was mixed with 100 mL of distilled water. As the mixture boiled for 20 min, the color of the aqueous solution was changed from watery to light yellow. After allowing the extract to cool down to room temperature, a Whatman filter paper broth filtration took place.

Preparation of zinc oxide NPs

30 mL of *Emblica Officinalis* leaves extract allowed to boil using a stirrer-heater. Then, 5 gm of zinc nitrate added to the solution at 60 °C. This mixture further boiled until its colour changed into deep yellow. This paste further transformed to the ceramic crucible and annealed at 400 °C for 2 h. The obtained light white coloured powder consumed for different characterizations.

Characterization of zinc oxide NPs

The UV-vis diffuse reflectance spectra (UV-vis-DRS) was recorded using a UV140404B model at the wavelength range of 200-850 nm in reflectance mode. PL spectra of the samples were also recorded using FLUOROLOG-FL3-11 fluorescence spectrometer. The crystalline structure of the samples was evaluated using a X-ray diffraction (XRD, model X'PERT PRO) diffractometer. FT-IR spectra recorded under identical conditions in the 400-4000 cm^{-1} region using fourier transform infrared spectrometer (SHIMADZHU). FE-SEM (JEOL JSM 6701-F) and TEM (JEM-2100) measurements revealed the morphology and size distribution.

Photocatalytic activity measurement

Photocatalytic activities of the ZnO nanoparticles were estimated from the degradation of methylene blue (MB) under UV irradiation. Heber multi-lamp photoreactor (HML MP 88) played its role in the study of degradation [25]. The dye of MB (10^{-4} M) with the appropriate amount of catalyst (20 mg) was stirred for 30 min in the dark prior to illumination. The progress of the reaction was monitored at different time intervals using Uv-visible Spectrophotometer. It is obvious that the intensity of blue colour of the reaction mixture decreased gradually and turned colourless at last. The absorbance for MB at 665 nm monitored with UV-vis spectrometer, was an indication of the catalytic activity of ZnO particles.

Antimicrobial assay

The synthesized compounds were tested for inhibition of the human pathogenic bacteria. Microbial assay was carried out using the disc diffusion method [26]. All the strains were enriched in nutrient broth at 37 °C for 18-24 h. Afterwards, they streaked over the surface of the Muller Hinton agar (MHA) using the sterile cotton swabs. Then, 20 µL of the extract was pipetted on a 6 mm sterile paper disc. Further, after the evaporation of the solvent, the disc placed over the surface of the plate, and the plates subjected incubation for 24 h at 37 °C. The usage of control discs with solvent specify the effect of solvent, and standard on pathogens. The halos (Zones) around the disc observed after 24 h displayed the amount of the growth inhibition.

Results and Discussion

XRD analysis

XRD patterns of the ZnO synthesized for different leaf extract levels (30-50 mL) are demonstrated in Figure 1. The diffraction peaks at $2\theta=31.25^\circ$, 33.91° , 36.04° , 47.03° , 56.07° , 62.35° , 65.84° , 68.43° , 72.06° and 76.43° correspond to (100), (002), (101), (102), (110), (103), (200), (112), (201), (004) and (202) planes, respectively. As indicated, all the diffraction patterns indexed to pure hexagonal wurtzite structured ZnO. The estimated lattice constants have values $a=b=3.25 \text{ \AA}$ and $c=5.21 \text{ \AA}$, which are close to the standard values (JCPDS no. 89-1397). The mean crystalline size (D) of the ZnO nanoparticles was calculated using the Equation 1 (Debye Scherrer's equation).

$$D = \frac{K\lambda}{\beta \cos\theta} \text{ \AA} \quad (1)$$

Where, $\lambda=1.5406 \text{ \AA}$ is the wavelength of the X-ray radiation used, θ is the Bragg diffraction angle, and β is the full width at half its maximum intensity of diffraction pattern (FWHM) in radian. The obtained sizes were found to be 44.58, 42.50 and 34.94 nm, respectively, for 30, 40, and 50 mL of extract addition. The results of the XRD analysis in this study are in agreement with the earlier report [27].

Optical studies

Figure 2a depicts the optical absorption spectra of the ZnO NPs synthesised by *Emblica Officinalis* extract. The sample had a clear and strong absorption peak below 400 nm. The band gap energy (E_g) of the ZnO was obtained from the wavelength value corresponding to the intersection point of the vertical and horizontal part of the spectrum, using the following equations:

$$E_g = \frac{hc}{\lambda} \text{ eV}; E_g = \frac{1240}{\lambda} \text{ eV} \quad (2)$$

where, E_g is the band gap energy (eV), h is the Planck's constant (6.626×10^{-34} Js), C is the light velocity (3×10^8 m/s), and λ is the wavelength (nm). As seen in [Figure 1a](#), the absorption edge were positioned at 363, 357 and 353 nm for 30, 40 and 50 mL extract concentration, respectively, which are corresponding to the band gap energy of 3.41, 3.47 and 3.51 eV. It was also found that, by increasing the extract concentration, the absorption peaks are red shifted in the UV region.

Indirect band gap energy (Kubelka-Munk plot)

The reflectance spectra were analyzed using the Kubelka-Munk relation (Equation 3). To convert the reflectance data into a Kubelka-Munk function (Equivalent to the absorption coefficient) $F(R)$, the following relation was used.

$$F(R) = \frac{(1-R)^2}{2R} \quad (3)$$

Where, R is the reflectance value. Band gap energy of the sample was estimated from the variation of the Kubelka-Munk function with photon energy. [Figure 2b](#) demonstrates the Kubelka-Munk plots for the ZnO NPs. It was used to determine their band gap energy associated with their indirect transitions. The ZnO exhibits indirect E_g of 3.39, 3.45 and 3.48 eV.

PL analysis

The PL properties of semiconducting materials are characterized with both intrinsic and extrinsic effects, which usually give rise to discrete electronic states in the band gap region and will influence the emission processes [28]. [Figure 3](#) depicts the PL emission spectrum of the ZnO recorded at the excitation wavelength of 325 nm. As seen in [Figure 3](#), the emission spectrum exhibits a strong UV emission at 412 nm and three weak visible emissions at 478, 492 and 528 nm. The strong UV emission at 412 nm can be ascribed to the recombination of excitons. The blue emissions at 478 nm, together with the blue green emission at 492 nm are probably from oxygen vacancies or other defects. The origin of green emission at 528 nm can be ascribed to the single ionized oxygen vacancies [29–31]. These oxygen vacancies are allowed to be recombine with the photo generated holes and resulted in green emission. From PL results, it is obvious that 50 mL of extract addition creates more oxygen vacancies.

FT-IR analysis

[Figure 4](#) illustrates the FT-IR analysis of both leaf extract and synthesized nanoparticles. The results may address the participatory compounds responsible for bio reduction. The appearance of

peaks at 3000-3500 cm^{-1} ascribed to OH stretching vibration of O-H groups in water, alcohol, and phenol.

Figure 1. XRD spectrum of ZnO NPs synthesized using *Emblica Officinalis* leaf extract.

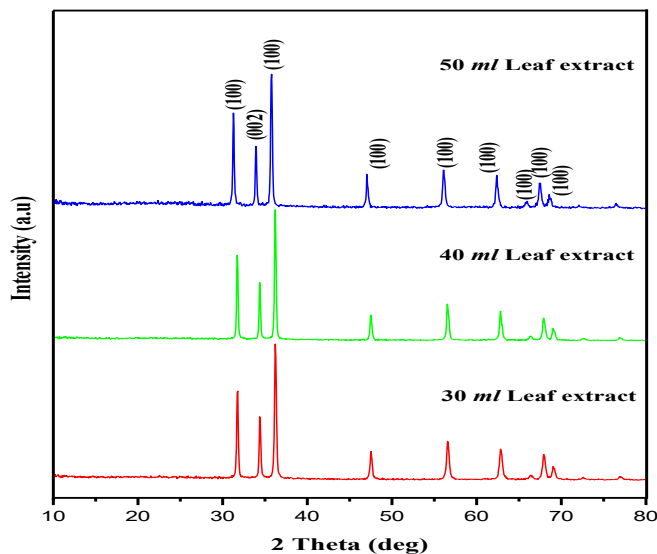


Figure 2a. UV-DRS spectrum of ZnO NPs synthesized using *Emblica Officinalis* leaf extract.

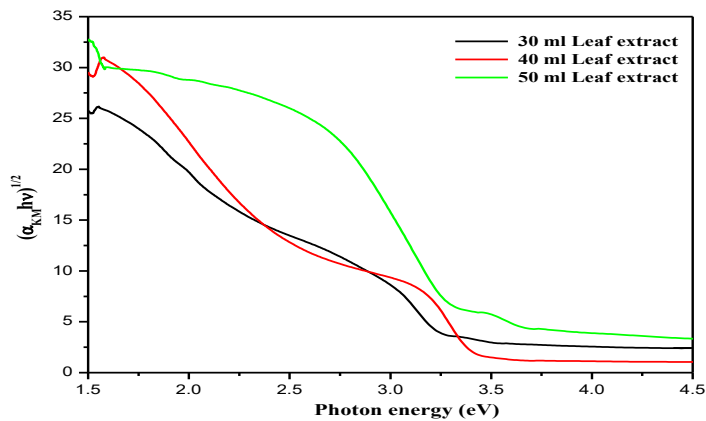
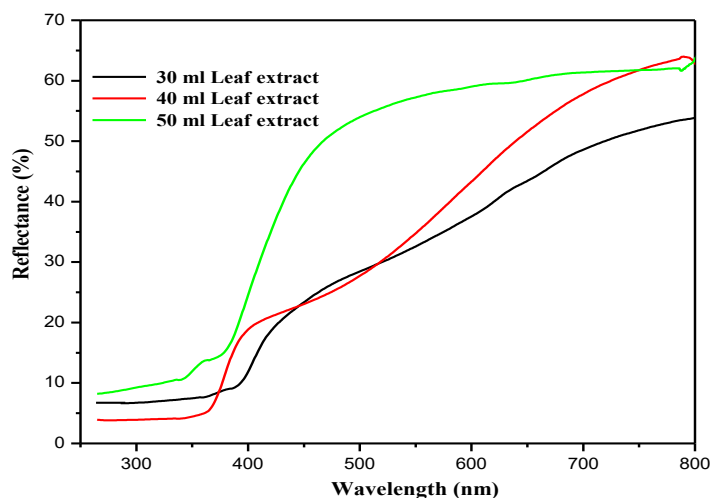


Figure 2b. Plot of indirect band gap energy for ZnO NPs.

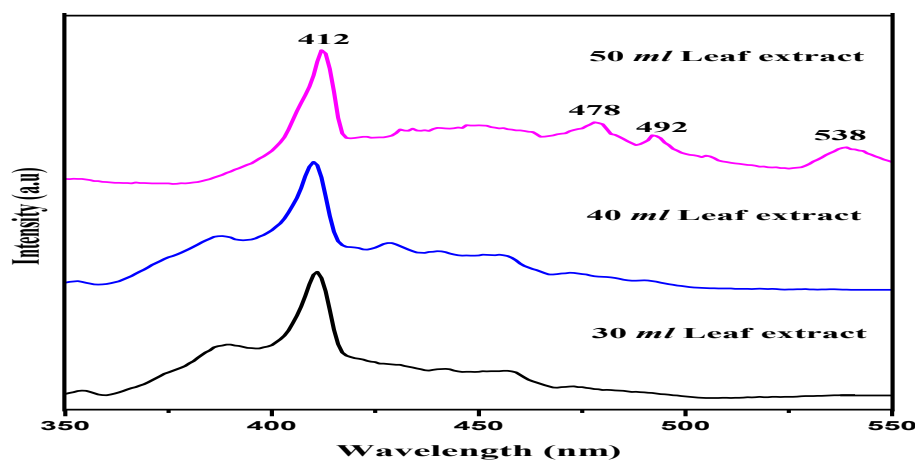


Figure 3. Photoluminescence spectrum of ZnO NPs synthesized using *Emblica Officinalis* leaf extract.

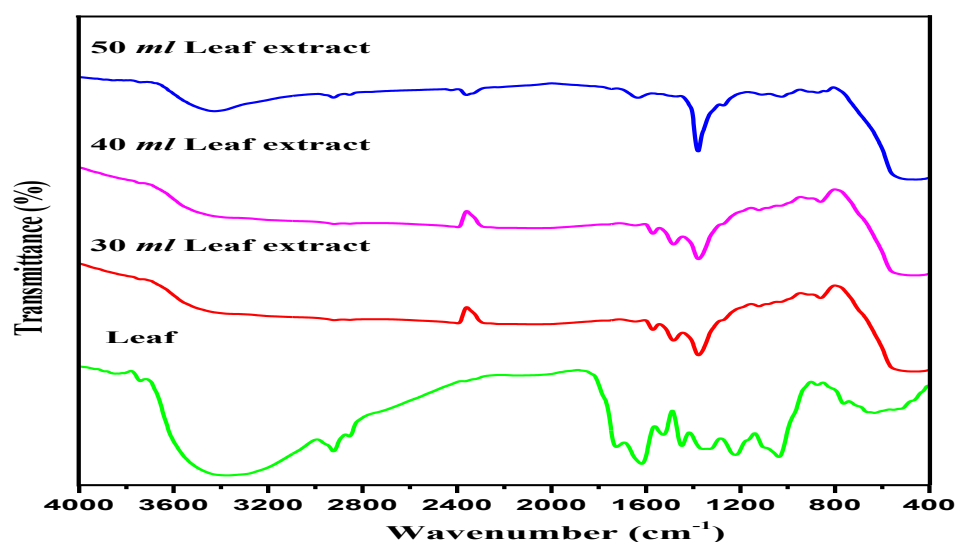


Figure 4. FT-IR spectra of leaf extract and ZnO NPs synthesized using *Emblica Officinalis* leaf extract.

The C–H stretching vibrations of alkanes and O–H stretching of carboxylic acid appeared at 2924 and 2854 cm^{-1} , respectively. The intense band at 1627 cm^{-1} was related to the C=C stretch in aromatic ring, and C=O stretch in polyphenols compounds [32]. The C=O bending of nitro groups gives the band at 1379 cm^{-1} [33]. A strong broad absorption peak appearing at 443 cm^{-1} can be ascribed to bending vibration of ZnO [34]. Thus, from the IR spectrum it is obvious that green tea sample was rich in polyphenols, carboxylic acid, polysaccharide, amino acid and proteins [35].

FE-SEM analysis

The synthesized ZnO nanoparticles from 50 mL addition of broth extract were analyzed for their morphology by field-emission scanning electron microscopy (FE-SEM). The FE-SEM images showed

the presence of plate-like structure (Figure 5a). Diameter of the cluster ZnO NPs found to be at the range of 20-40 nm. From the EDX pattern (Figure 5b) the existence of elements Zn and O was confirmed.

TEM analysis

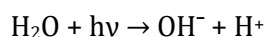
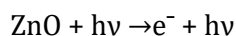
The TEM micrograph of the ZnO (50 mL of broth addition) further evaluated the morphology and size of the synthesized product. Figure 6 reveals that most of the ZnO NPs are quasi-spherical (Figure 6a) with the particle size of 30-40 nm (Figure 6c). The SAED pattern (Figure 6b) shows the well defined electron diffraction spots, confirming the single crystalline nature of the quasi-spherical of ZnO nanocrystals.

Photocatalytic activity

It is well-known that the catalytic activity of the NPs strongly depends on its composition, size, and shape. Photocatalytic activity of the ZnO NPs (50 mL of extract) was investigated by selecting the photocatalytic degradation of methylene blue. However, when the experiment was carried out by the introduction of ZnO NPs, the color of the solution was changed from blue to colorless. The ultraviolet-visible (UV-vis) absorption results of an aqueous solution of methylene blue checked in the presence of ZnO NPs at different time intervals. The absorption peak decreased gradually with the extension of the exposure times, indicating the photocatalytic degradation [36–39].

Probable mechanism for photodegradation of methylene blue (MB) using synthesized ZnO NPs

When the surface of the ZnO NPs irradiated with light, the electron (e^-) from the valence band of ZnO, moved to the conduction band and thereby leaving a hole (h^+) in the valence band. The holes (h^+) act as an oxidizing agent and oxidize the pollutant directly, or they may react with water to provide hydroxyl radicals. The electron (e^-) in the conduction band performs as reducing agent that reduces the oxygen adsorbed on the surface of ZnO photocatalyst. Further, after irradiation the dye gets excited and the excited dye injected an electron to the conduction band of ZnO and scavenged by pre-adsorbed oxygen, to form active oxygen radicals. These generated active radicals that drove the photodegradation process. The ZnO nanoparticles play an important role as an electron carrier. The reasonable mechanism for the photocatalytic degradation of MB dye can be schematically shown as [40].



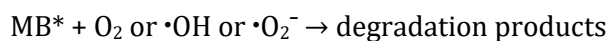
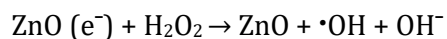
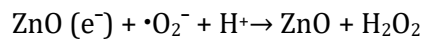
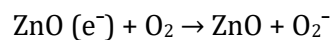
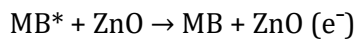
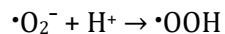
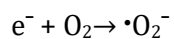
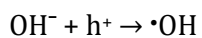
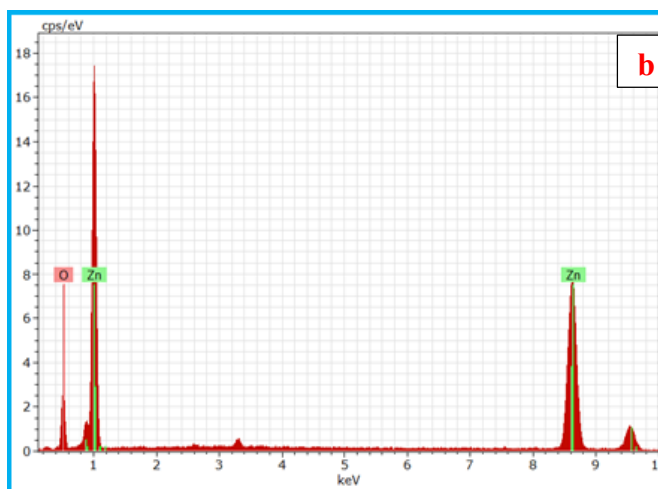
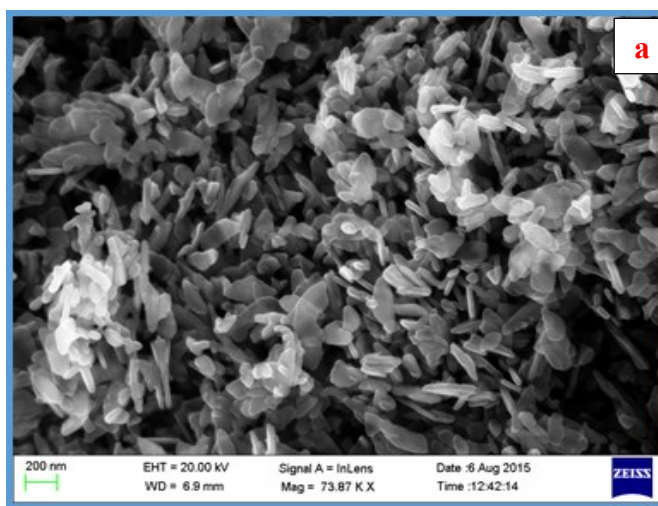


Figure 5. FE-SEM image and EDX spectrum of the ZnO NPs synthesized using 50 mL of *Emblica Officinalis* leaf extract.



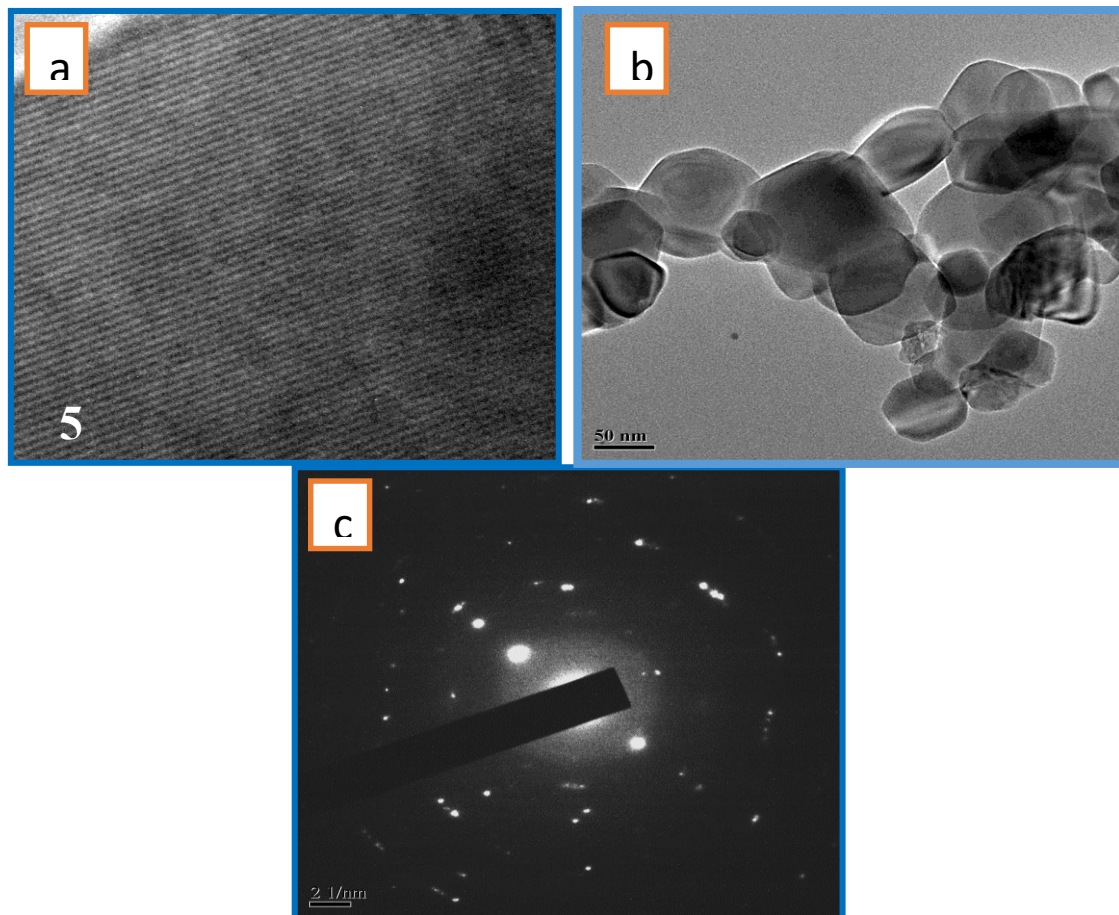


Figure 6. a) TEM image ZnO NPs synthesized using 50 mL of *Emblica Officinalis* leaf extract, b) corresponding SAED patterns and c) Particle size histogram

Antibacterial activity of ZnO NPs

Antibacterial activity of the green synthesized ZnO NPs (50 mL of extract) towards various human pathogens was tested using the disc diffusion methods (Figures 7 and 8). The antibacterial activity of leaf mediated ZnO was studied against the gram-negative and the gram-positive bacteria. As seen in the Figure 8, inhibition zones of 6 mm, 10 mm, 7 mm, and 9 mm were obtained from the synthesized ZnO nanoparticles against *S. paratyphi*, *V. cholerae*, *S. aureus*, and *E. coli*, respectively. In the present study, when compared to leaf extract and solvent, green synthesized ZnO NPs showed a greater significant zone of inhibition. However, when compared to the standard tablet, lower antibacterial activity of the ZnO NPs was observed in all the bacterial pathogens. The results of the present study were found to be identical with the results reported by other researchers [41–44]. The potential reason for the antibacterial activity of ZnO is that the ZnO NPs may attach to the surface of the cell membrane and perturbing the permeability and respiration functions of the cell. Smaller ZnO NPs

can have larger surface area available for interaction and may give more antibacterial effect than the larger particles. It is also possible that the ZnO NPs not only interact with the surface of the membrane, but can also penetrate inside the bacteria.

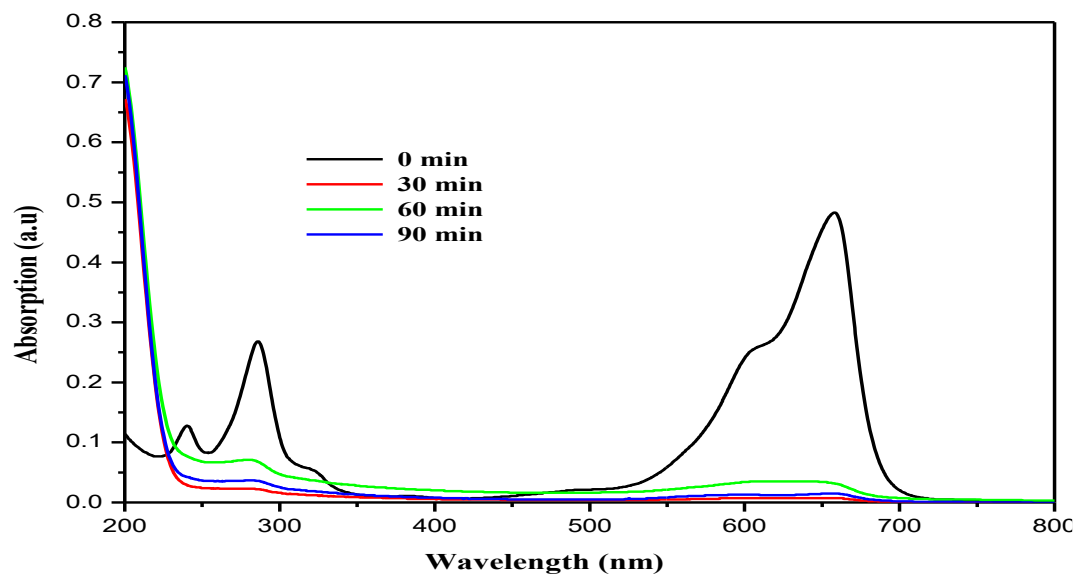


Figure 7. UV-Visible spectra of methylene blue reduction by 50 mL of *Emblica Officinalis* in the presence of ZnO NPs.

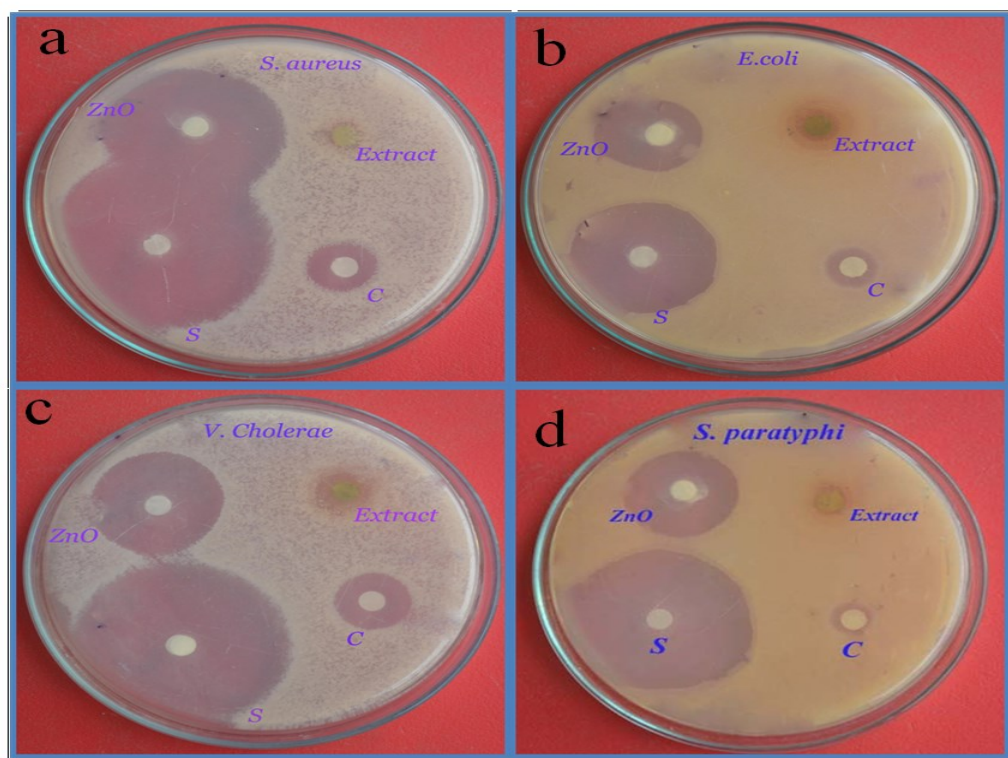


Figure 8. Antibacterial activity of ZnO NPs synthesized using 50 ml of *Emblica Officinalis* leaf extract

Conclusion

In this work, we have suggested a simple green synthesis method to prepare the ZnO nanoparticles using different amounts of *Emblica Officinalis* leaf extract. The diffraction patterns reveal that the particle size could be controlled by adjusting the amount of leaf extract addition. The photocatalytic performance of the green synthesized ZnO showed its enhanced activity against the organic dye methylene blue under UV irradiation. In addition, the prepared ZnO nanoparticles revealed potential antibacterial activities against the pathogens subjected for analysis. The results also showed that, the *Emblica Officinalis* leaf extract assisted photocatalytic activity of ZnO analyzed against green at the presence of UV irradiation and revealed its enhanced performance in the mixed phase.

Acknowledgements

The authors are thankful to the Department of Physics, Annamalai University, Tamilnadu-608 002 and Sri Akilandeswari Women's College, Wandiwash, Tamil Nadu, India - 604 408 for providing all necessary facilities to carry out the present work .

Disclosure Statement

No potential conflict of interest was reported by the authors.

References

- [1]. Das S.N., Kar J.P., Choi J.H., Lee T.I., Moon K.J., Myoung J.M. *J. Phys. Chem. C*, 2010, **114**:1689
- [2]. Huang M.H., Mao S., Feick H., Yan H., Wu Y., Kind H., Weber E., Russo R., Yang P. *Science*, 2001, **292**:1897
- [3]. Wang Z.S., Huang C.H., Huang Y.Y., Hou Y.J., Xie P.H., Zhang B.W., Cheng H.M. *Chem. Mater.*, 2001, **13**:678
- [4]. Liu Z., Liu C., Ya J., Lei E. *Renew. Energy*, 2011, **36**:1177
- [5]. Lee C.J., Lee T.J., Lyu S.C., Zhang Y., Ruh H., Lee H.J. *Appl. Phys. Lett.*, 2002, **81**:3648
- [6]. Sridevi D., Rajendran K.V. *Bull. Mater. Sci.*, 2009, **32**:165
- [7]. Honma I., Hirakowa S., Yamada K., Bae J.M. *Solid State Ionics*, 1999, **118**:29
- [8]. Zeng J.H., Jin B.B., Wang Y.F. *Chem. Phys. Lett.*, 2009, **472**:90
- [9]. Arumugam A., Karthikeyan C., Syedahamed Haja Hameed A., Gopinath K., Gowri S., Karthika V. *Mater. Sci. Eng.*, 2015, **49**:408
- [10]. Sangeetha G., Rajeshwari S., Venckatesh R. *Mater. Res. Bull.*, 2011, **46**:2560
- [11]. Azizi S., Ahmad M.B., Namvar F., Mohamad R. *Mater. Lett.*, 2014, **116**:275

- [12]. Sangeetha N., Kumaraguru A.K. *J. Nanobiotechnol.*, 2013, **11**:39
- [13]. Jayaseelan C., Abdul Rahuman A., Vishnu Kirthi A., Marimuthu S., Santhoshkumara T., Bagavana A., Gaurav K., Karthik L., Bhaskara Rao K.V. *Spectrochim. Acta A*, 2012, **90**:78
- [14]. Rajiv P., Rajeshwari S., Venckatesh R. *Spectrochim. Acta A*, 2013, **112**:384
- [15]. Mahre M.B., Umaru B., Ojo N.A., Yahi D., Sa'idu A.S., Musa A.S., Bukola O.O. *J. of Research in Forestry, Wildlife & Enviro.*, 2017, **9**:2141
- [16]. Vidya C., Hirematha S., Chandraprabha M.N., Lourdu Antonyraja M.A., Venu Gopal I., Jaina A., Bansala K. *Int. J. Curr. Eng. Technol.*, 2013, **2277**:118
- [17]. Ain Samat N., Md Nor R. *Ceram. Int.*, 2013, **39**:S545
- [18]. Gnanasangeetha D., Saralathambavani D. *Asian Acad. Res. J. Multidiscip.*, 2013, **1**:164
- [19]. Vivekanandhan S., Schreiber M., Mason C., Mohanty A.K., Misra M. *Colloids Surf. B: Biointerfaces.*, 2014, **113**:169
- [20]. Elumalai K., Velmurugan S., Ravi S., Kathiravan V., Ashokkumar S. *Spectrochim. Acta A*, 2015, **136**:1052
- [21]. Ramesh M., Anbuvarannan M., Viruthagiri G. *Spectrochim. Acta A*, 2015, **136**:864
- [22]. Anbuvarannan M., Ramesh M., Viruthagiri G., Shanmugam N., Kannadasan N. *Mat. Science Semiconduct. Process.*, 2015, **39**:621
- [23]. Anbuvarannan M., Ramesh M., Viruthagiri G., Shanmugam N., Kannadasan N., *Spec. Acta Part A: Molecul. Biomolecul. Spectr.*, 2015, **14**:304
- [24]. Anbuvarannan M., Ramesh M., Manikandan E., Srinivasan R. *Asian J. of Nanosci and Mat.*, 2018, **2**:99
- [25]. Senthilraja A., Subash B., Krishnakumar B., Rajamanickam D., Swaminathan M., Shanthi M. *Mat. Sci. Semiconductor Proc.*, 2014, **22**:83
- [26]. Kelman D., Kashman Y., Rosenberg E., Ilan M., Iirach I., Loya Y. *Aquat. Microb. Ecol.*, 2001, **24**:9
- [27]. Sangeetha G., Rajeshwari S., Venckatesh R. *Mater. Res. Bull.*, 2011, **46**:2560
- [28]. Vanheusden K.V., Warren W.L., Seager C.H. *J. Appl. Phys.*, 1996, **79**:7983
- [29]. Heo Y.W., Norton D.P., Pearton S.J. *J. Appl. Phys.*, 2005, **98**:073502
- [30]. Lin B., Fu Z., Jia Y. *Appl. Phys. Lett.*, 2001, **79**:943
- [31]. Huang M.H., Wu Y., Feick H., Tran N., Weber E., Yang P. *Adv. Mater.*, 2001, **13**:113
- [32]. Anbuvarannan M., *Inter. J. of Recent Scientific Research.*, 2017, **8**:18501
- [33]. Senthilkumar S.R., Sivakumar T. *Int. J. Pharm. Pharmaceutical Sci.*, 2014, **6**:461
- [34]. Deng Y., Wang G., Li N., Guo L. *J. Luminescence.*, 2009, **129**:55
- [35]. Anbuvarannan M., *Inter. J. of Recent Scientific Research.*, 2017, **8**:19224

- [36]. Ngoc Tien H., Hoang Luan V., Thuy Hoa L., Tri Khoa N., Hong Hahn S., Suk Chung J., Woo Shin E., Hyun Hur S. *Chem. Eng. J.*, 2013, **229**:126
- [37]. Nipane S.V., Korake P.V., Gokavi G.S. *Ceramics Int.*, 2015, **41**:4549
- [38]. Pirhashemi M., Habibi-Yangjeh A. *App. Surface Sci.*, 2013, **283**:1080
- [39]. Zaman M.S., Haberer E.D. *J. App. Phy.*, 2014, **116**:154308
- [40]. Anbuvarannan M., Ramesh M., Viruthagiri G., Shanmugam N., Kannadasan N. *Spectro. Acta Part A: Molecul. Biomolecul. Spec.*, 2015, **143**:304
- [41]. Gunalana S., Sivaraja R., Rajendran V. *Prog. Nat. Sci. Mater. Int.*, 2012, **22**:693
- [42]. Manjunath K., Ravishankar T.N., Kumar D., Priyanka K.P., Varghese T., Raja Naika H., Nagabhushana H., Sharma S.C., Dupont J., Ramakrishnappa T., Nagaraju G. *Mater. Res. Bul.*, 2014, **57**:325
- [43]. Shinde V.V., Dalavi D.S., Mali S.S., Hong C.K., Kim J.H., Pramod Patil P.S. *App. Surface Sci.*, 2014, **307**:495
- [44]. Jan T., Iqbal J., Ismail M., Mansoor Q., Mahmood A., Ahmad A. *App. Surface Sci.*, 2014, **308**:75

How to cite this manuscript: Anbuvarannan Mari*, Ramesh Mookkaiah, Manikandan Elayaperumal. *Emblica officinalis* leaf extract mediated synthesis of zinc oxide nanoparticles for antibacterial and photocatalytic activities. *Asian Journal of Green Chemistry*, 3(4) 2019, 418-431. DOI: [10.33945/SAMI/AJGC.2019.4.1](https://doi.org/10.33945/SAMI/AJGC.2019.4.1)